Revista Mexicana de Astronomía y Astrofísica, **46**, 89–107 (2010)

THE GREEN POTENTIAL OF THE SAN PEDRO MÁRTIR OBSERVATORY

J. Bohigas and J. M. Núñez
Instituto de Astronomía, Universidad Nacional Autónoma de México, Mexico

Received 2009 September 17; accepted 2009 November 23

RESUMEN

Se analizan observaciones meteorológicas realizadas entre octubre 2004 y julio 2008 en el Observatorio Astronómico Nacional de México (OAN). En abril, mayo y junio la humedad fue inferior a 55% casi 90% del tiempo. La velocidad del viento fue mayor durante la noche y disminuyó entre marzo y noviembre. Las variaciones nocturnas, diarias y anuales de temperatura fueron cercanas a 2, 6 y 16°C, respectivamente. La altura de escala para la función que relaciona la velocidad del viento con la altura sobre el suelo está entre 0.55 y 0.67 metros. La operación normal del OAN produjo algo más que 750 toneladas de CO_2^{eq} al año, unas 3 veces más que las emitidas por una industria mediana típica del municipio de Ensenada, donde está ubicado el OAN. La energía eólica pudo ser utilizada para producir electricidad $\sim 60\%$ del tiempo, siendo más abundante durante la noche y en los meses de invierno y primavera temprana. La energía solar y eólica parece bastar para cubrir todas las necesidades energéticas del observatorio, cerca de 110 kWh, incluyendo transporte.

ABSTRACT

Weather observations carried out between October 2004 and July 2008 at the Mexican Observatorio Astronómico Nacional (OAN) are analyzed. Humidity in April, May and June was less than 55% nearly 90% of the time. Wind speed was larger at nightime and tended to decrease between March and November. Typical temperature variations during the night, for the entire day and for a whole year were about 2, 6 and 16°C, respectively. The scale height or roughness length for the function relating wind speed and height above ground is between 0.55 and 0.67 meters. Normal activities associated to OAN produced somewhat more than 750 tons of CO_2^{eq} a year, roughly 3 times more than a typical mid-scale industry in the district of Ensenada, where OAN is located. Wind energy could have been extracted to produce electricity $\sim 60\%$ of the time, being more bountiful during the night and in the winter and early spring months. Solar and wind energy seem plentiful enough to supply the entire energy needs of the observatory, some 110 kWh including transportation.

Key Words: seeing — site testing

1. INTRODUCTION

There has been very little systematic long and mid-term monitoring of weather variables at the Mexican Observatorio Astronómico Nacional (hereafter OAN) at the Sierra de San Pedro Mártir (hereafter SPM), Baja California. Until very recently, efforts to produce weather reports have been the task of a few individuals, but their observations have been confined to brief periods of time or to qualitative descriptions of a few parameters. Accounts of these activities can be found in Álvarez et al. (2007) and Tapia et al. (2007). In spite of this, or perhaps because of this, these incomplete reports have been of great value to assess the virtues and defects of San Pedro Mártir as an astronomical site.

OAN is located at 115° 28″ W and 31° 3″ N at an altitude between 2700 and 2800 meters (see `haro.astrossp.unam.mx/indexspm.html`). It is well within the northern subtropical high pressure belt. At this latitude the weather is characterized by low cloud cover and precipitation, and weak and erratic sea level surface winds. In Baja California

TABLE 2

	2004		2005		2006		2007		2008	
Month	Days	Records	Days	Records	Days	Records	Days	Records	Days	Records
January	0	0	23	16034	24	16652	23	15043	0	0
February	0	0	28	20111	28	19367	28	19824	14	9898
March	0	0	31	21633	10	6480	23	15391	31	21689
April	0	0	30	21527	0	0	13	8581	30	21364
May	0	0	31	19947	11	6869	31	21844	31	21907
June	0	0	30	20852	30	20848	24	14318	30	21083
July	0	0	28	19559	26	18226	31	22161	29	20175
August	0	0	0	0	27	17774	31	21928	0	0
September	0	0	0	0	30	21463	1	364	0	0
October	29	19899	25	17846	31	21926	21	14998	0	0
November	30	21487	30	21490	29	19368	28	19907	0	0
December	20	13855	17	11644	18	11646	17	10826	0	0

TMT weather station. Number of working days and valid records for atmospheric temperature, pressure, humidity and solar irradiance (set VT).

TABLE 1

Weather variable	Range	Accuracy
Wind velocity (m/s)	0.1 to 40	±2%
Pressure (hPa)	600 to 1100	±5%
Relative humidity (%)	0 to 100	±2%
Solar radiation (w/m^2)	0 to 2000	±5%
Temperature (°C)	−40 to +60	±0.1°C
Wind direction (°)	0 to 360	±1°

TMT weather station. Certified sensor range and accuracy.

wind velocity picks up in the mountain ranges that run along the peninsula, among them SPM (see `www.nrel.gov/wind/pdfs/mexico-baja.pdf`). Tropical cyclones, which frequently land on the southern end of the peninsula, can affect the weather at OAN during the late summer and early autumn months. Extratropical cyclones over the north Pacific are formed during the winter months, and these are the main source of precipitation.

Satellite observations confirmed local reports on the exceptionally large fraction of photometric nights at SPM (Erasmus & van Staden 2002). This condition prompted the Site Selection Team of the Thirty Meter Telescope Project (hereon TMT, at www.tmt.org) to carry out an extensive inspection of weather and seeing variables at San Pedro Mártir, among a small host of other promising sites. Additionally, the Site Selection Team of the Large Synoptic Survey Telescope, or LSST (at `www.lsst.org`),

TABLE 3

	T	H	V	P
Max	26.8	100	117.5	743.4
Min	−13.3	2	0.0	697.0
Average	8.0	45	9.0	734.2
σ	6.8	24	7.1	nan
Mode	7.7	100	0.0	733.8
O1	−0.3	20	2.3	727.3
Q1	3.2	25	4.2	729.8
O3	5.8	35	5.7	731.8
Median	8.3	37	7.4	733.5
O5	10.8	45	9.4	735.0
Q3	13.2	58	12.1	736.5
O7	15.8	78	16.6	738.1

TMT weather station. Statistics for temperature (T in °C), relative humidity (H as a %), wind speed (V in km/h) and pressure (P in hPa) between October 2004 and July 2008. Symbols O1, O3, O5 and O7 stand for the first, third, fifth and seventh octiles of the distribution, whereas Q1 and Q3 stand for the first and third quartile.

installed an all sky camera and a 30 meter tower with 4 ultrasonic anemometers at SPM, in order to complement and share the observations that were being conducted for TMT. TMT and LSST own most of the equipment that was used at SPM to carry out these measurements, but manpower was provided by these two institutions as well as OAN. The LSST project finished their site assessment in 2006, and

TABLE 4

	T	H	V	P	T	H	V	P	T	H	V	P
	Jan				Feb				Mar			
Max	13.7	100	79.9	740.3	16.7	100	67.3	738.9	17.5	100	117.5	738.7
Min	−13.3	12	0.0	719.9	−13.1	11	0.0	717.9	−11.8	12	0.0	713.1
Average	0.3	47	10.2	730.2	1.3	52	12.1	729.8	3.5	40	10.5	731.0
σ	5.0	27	8.5	6.4	5.0	31	7.6	nan	4.9	24	7.3	9.3
Mode	−1.6	100	0.0	728.8	1.6	100	0.0	727.3	4.5	100	0.0	733.6
O1	−5.9	20	2.1	725.0	−4.8	18	4.5	725.1	−2.3	18	3.9	726.3
Q1	−2.9	25	4.4	727.1	−2.5	24	6.6	726.7	0.0	22	5.4	728.4
O3	−1.0	36	6.3	728.7	−0.4	36	8.5	728.0	2.1	27	7.0	729.9
Median	0.5	38	8.3	730.2	1.5	40	10.6	729.6	3.6	36	8.8	731.5
O5	2.3	48	10.9	731.7	3.1	57	13.0	731.4	5.2	37	11.0	733.0
Q3	4.1	64	14.2	733.6	4.9	88	15.9	732.8	7.1	46	13.8	734.2
O7	5.8	90	19.6	735.3	7.4	100	20.6	735.3	9.2	72	18.5	735.7
	Apr				May				Jun			
Max	18.4	100	66.0	738.1	24.7	100	63.7	740.4	25.3	99	53.3	743.2
Min	−11.0	12	0.0	718.5	−7.1	12	0.0	713.2	3.2	11	0.0	725.8
Average	5.9	36	10.5	731.1	9.4	38	9.0	731.8	14.7	35	9.0	735.7
σ	4.4	18	6.6	nan	4.9	16	6.0	6.9	3.6	14	5.6	5.4
Mode	6.0	100	0.0	731.4	8.3	100	0.0	733.3	14.1	36	0.0	739.2
O1	1.0	18	3.9	727.6	3.9	20	3.5	727.9	10.6	19	3.7	731.8
Q1	3.0	23	5.5	728.9	6.1	26	4.8	729.7	12.1	24	5.1	733.6
O3	4.4	26	7.1	730.1	7.9	35	6.1	731.1	13.3	28	6.4	734.8
Median	6.0	34	9.0	731.1	9.5	36	7.4	732.4	14.4	35	7.7	736.0
O5	7.3	36	11.1	732.0	10.9	39	9.1	733.4	15.7	36	9.4	737.1
Q3	9.0	42	13.9	733.5	12.8	45	11.5	734.4	17.4	41	11.5	738.1
O7	11.0	54	18.4	735.0	14.9	55	15.6	735.9	19.3	51	15.0	739.3

TMT weather station. Typical month statistics for temperature (T in °C), relative humidity (H as a %), wind speed (V in km/h) and pressure (P in hPa) for January, February, March, April, May and June, between October 2004 and July 2008. Symbols O1, O3, O5 and O7 stand for the first, third, fifth and seventh octiles of the distribution, whereas Q1 and Q3 stand for the first and third quartile.

sometime later decided for Cerro Pachón in Chile. TMT stayed at SPM until the end of July 2008, and a year later determined to construct at Mauna Kea.

In § 2 we analyze atmospheric temperature, pressure, humidity and wind speed and direction at SPM between October 2004 and July 2008. This is the longest continuous monitoring campaign of these parameters at SPM. Using data from the four ultrasonic anemometers installed at a 30 meter tower, in § 3 we determine wind velocity as a function of height up to a distance of ∼ 30 meters from ground level, a useful tool for engineering design among other things. We estimate the energy use and carbon footprint of OAN in § 4, taking for granted that this is an important excercise given the difficult circumstances that are expected from global warming. Using the solar irradiation and weather data at our disposal, in § 5 we consider the posibility of substituting carbon based energy sources at OAN with solar and wind energy. Conclusions are given in § 6. A large number of tables and figures has been included to support our analysis.

2. RESULTS FROM THE TMT WEATHER STATION

The TMT site selection team inspected weather and seeing conditions at SPM between October 2004 and July 2008, at a site commonly known as "TIM" or "Cerro Pelado" (see Bohigas et al. 2008 and Schöck et al. 2009). They used a Monitor Sensors weather station (at `www.monitorsensors.com`), producing one minute averages of atmospheric temperature, humidity, pressure, wind velocity and direction and solar irradiation between 400 and 950 nanometers (see Riddle et al. 2009, in preparation), every two minutes. Range and accuracy for each sensor, as given by the manufacturer, are presented in Table 1.

Incorrect or dubious records, such as out-of-order time stamps or data values that are out of the sen-

TABLE 5

	T	H	V	P	T	H	V	P	T	H	V	P
	Jul				Aug				Sep			
Max	26.8	100	41.0	742.7	24.1	100	41.1	742.2	19.6	100	80.8	741.4
Min	9.5	13	0.0	733.0	8.0	14	0.0	697.0	2.7	14	0.0	728.1
Average	16.2	56	7.2	738.3	14.7	62	7.4	736.9	11.7	61	12.6	735.2
σ	3.3	23	4.1	2.7	2.6	17	3.8	9.2	2.6	25	11.2	0.7
Mode	15.5	100	0.0	738.2	13.3	100	0.0	736.9	11.8	100	0.0	735.7
O1	12.5	27	3.2	736.5	12.0	40	3.3	735.6	8.9	34	0.0	731.9
Q1	13.7	37	4.4	737.2	12.9	49	4.7	736.3	9.9	40	3.3	733.8
O3	14.8	47	5.4	737.7	13.6	56	5.8	736.8	10.7	50	7.2	734.8
Median	15.7	56	6.5	738.2	14.3	62	6.9	737.3	11.6	61	10.9	735.5
O5	16.9	64	7.7	738.7	15.3	68	8.1	737.8	12.5	71	14.8	736.1
Q3	18.3	72	9.3	739.4	16.6	74	9.5	738.4	13.6	79	19.3	736.9
O7	20.4	84	11.7	740.1	18.1	83	11.7	739.1	14.9	100	25.6	738.5
	Oct				Nov				Dec			
Max	19.4	100	107.9	741.3	18.3	100	59.9	741.6	17.3	100	64.1	743.4
Min	−5.7	12	0.0	719.3	−10.3	2	0.0	701.3	−10.3	12	0.0	712.0
Average	8.0	44	8.0	731.8	6.2	39	6.5	732.1	2.7	42	8.7	731.4
σ	4.3	23	9.3	nan	4.7	23	6.7	nan	5.1	27	7.4	5.4
Mode	7.7	100	0.0	731.5	6.6	100	0.0	734.7	5.5	100	0.0	735.3
O1	3.0	20	0.0	726.7	0.7	17	0.0	727.1	−3.6	18	0.0	724.6
Q1	5.1	26	1.4	729.1	3.3	22	1.1	729.9	−0.4	22	3.0	729.1
O3	6.8	35	3.0	730.8	5.2	27	2.9	731.7	1.3	26	5.3	730.6
Median	8.4	38	5.0	732.1	6.7	36	4.8	733.0	3.0	36	7.5	732.3
O5	9.7	46	7.7	733.3	8.0	37	7.0	734.0	4.7	37	9.8	733.8
Q3	10.9	54	11.6	734.6	9.4	47	10.0	735.0	6.3	48	12.6	735.1
O7	12.8	71	17.8	736.1	11.4	65	14.4	736.2	8.3	95	16.9	736.6

TMT weather station. Typical month statistics for temperature (T in °C), relative humidity (H as a %), wind speed (V in km/h) and pressure (P in hPa) for July, August, September, October, November and December, between October 2004 and July 2008. Symbols O1, O3, O5 and O7 stand for the first, third, fifth and seventh octiles of the distribution, whereas Q1 and Q3 stand for the first and third quartile.

sor range or beyond extreme atmospheric conditions, were detected and removed. In Table 2 we present the number of monthly working days and valid records produced by the TMT weather station for all variables except wind speed and direction (data set VT). Set VT includes 727,792 records registered during 1052 days. As can be seen from Table 2, weather variables were measured for at least 3 years in all months except August and September.

Wind speed and direction measurements are impossible when ice, snow or dust buildup prevents the motion of these mechanical sensors. These failures are only evident when the weather station registers nearly constant wind direction and/or zero wind speed for long periods of time, i.e. more than a day. We found that the anemometer was probably out of service between February 9 and March 4, 2005, and between August 26 and September 6, 2006. Thus, wind speed statistics were obtained for a set (set V0) where the number of days and records for February 2005, March 2005, August 2006 and September 2006 are (9, 6233), (27, 18733), (21, 13469) and (25,17860) respectively. Set V0 includes 703,106 records registered during 1018 days. The wind direction is very variable when the wind speed is very small. Thus, wind direction statistics are available for a set (hereafter set V1) where the wind speed is larger than 0.1 km/hr (or 0.03 m/s, 3 times less than the guaranteed lower limit). Set V1 includes 652,180 records registered during 1016 days. Notice too that the weather station was standing just 2 meters above ground level, so that the wind may have been deflected and slowed down by treetops standing $\sim$ 30 meter away from the station (the area had been cleared).

Statistics for all weather variables (except wind direction and solar irradiation) between October 2004 and July 2008 are presented in Table 3. Statistics for "typical" months during this period are shown in Tables 4 and 5, and average, mode and median monthly values for temperature, wind speed

TABLE 6

	T	H	V	P	T	H	V	P	T	H	V	P	T	H	V	P
	SR-				SR+				MD-				MD+			
Max	24.0	100	80.8	741.9	21.5	100	88.6	742.5	26.6	100	107.9	743.4	26.8	100	117.5	743.1
Min	−13.2	2	0.0	701.3	−13.1	12	0.0	702.4	−11.9	12	0.0	701.9	−11.1	12	0.0	703.0
Average	5.8	45	9.7	732.1	6.3	44	9.4	732.6	10.4	42	8.1	734.0	11.7	44	7.6	733.5
σ	6.2	25	7.7	3.1	6.1	25	7.6	4.5	6.7	22	6.8	10.6	6.6	22	6.3	11.5
Mode	4.8	100	0.0	734.4	5.3	100	0.0	733.6	8.2	100	0.0	734.8	9.2	100	0.0	735.1
O1	−1.6	18	1.7	726.5	−1.3	18	1.5	726.9	2.1	20	1.8	728.4	3.5	23	1.7	728.2
Q1	1.4	24	4.6	729.0	2.0	23	4.2	729.5	5.8	24	3.7	731.0	7.6	28	3.6	730.6
O3	3.8	35	6.5	730.9	4.4	35	6.2	731.5	8.6	30	5.1	733.1	10.1	36	5.0	732.5
Median	6.1	37	8.3	732.7	6.6	37	8.1	733.2	11.1	36	6.6	734.7	12.4	37	6.4	734.3
O5	8.3	46	10.4	734.1	9.0	45	10.1	734.6	13.4	41	8.3	736.2	14.4	44	8.0	735.8
Q3	10.9	60	13.3	735.7	11.5	58	12.8	736.1	15.6	52	10.8	737.6	16.7	54	10.1	737.1
O7	13.0	81	17.9	737.1	13.6	81	17.5	737.6	18.0	69	15.0	739.1	19.1	73	13.9	738.7
	SS-				SS+				MN-				MN+			
Max	24.4	100	78.0	741.8	20.8	100	98.1	742.1	20.3	100	73.4	742.7	20.6	100	95.5	742.4
Min	−11.1	11	0.0	700.7	−11.4	11	0.0	697.1	−13.3	11	0.0	697.0	−12.3	11	0.0	702.7
Average	8.6	48	7.2	732.6	6.8	49	8.2	732.5	5.8	45	9.3	732.6	5.4	44	9.8	731.9
σ	6.3	23	6.5	5.3	6.1	25	6.9	5.1	6.1	25	7.5	9.3	6.1	26	7.9	6.8
Mode	7.9	100	0.0	734.9	6.5	100	0.0	733.9	6.6	100	0.0	733.8	6.6	100	0.0	733.0
O1	0.7	23	1.0	727.3	−0.6	21	1.2	727.2	−1.7	18	1.1	727.2	−1.8	18	1.3	726.4
Q1	4.2	34	2.9	729.7	2.6	28	3.4	729.5	1.6	24	4.0	729.6	1.3	23	4.3	728.9
O3	6.9	36	4.3	731.5	4.9	36	5.0	731.3	3.9	35	6.0	731.5	3.5	34	6.3	730.8
Median	9.0	41	5.7	733.2	6.9	43	6.6	733.0	6.0	37	7.9	733.1	5.7	37	8.2	732.6
O5	11.3	50	7.4	734.7	9.3	52	8.7	734.6	8.1	47	10.1	734.6	7.7	46	10.5	733.9
Q3	13.6	61	9.8	736.1	11.8	65	11.5	736.1	10.6	61	13.0	736.1	10.1	58	13.6	735.5
O7	15.9	81	14.2	737.5	13.9	85	15.9	737.5	13.3	81	17.6	737.6	12.9	82	18.4	737.0

TMT weather station. Typical day statistics for temperature (T in °C), relative humidity (H as a %), wind speed (V in km/h) and pressure (P in hPa). Symbols O1, O3, O5 and O7 stand for the first, third, fifth and seventh octiles of the distribution, whereas Q1 and Q3 stand for the first and third quartile. SR- and SR+ extend for 1.5 hours before and after sunrise, SS- and SS+ extend for 1.5 hours before and after sunset, MD- and MD+ are the first and second part of the day (equally divided) and MN- and MN+ are before and after midnight (also equally divided).

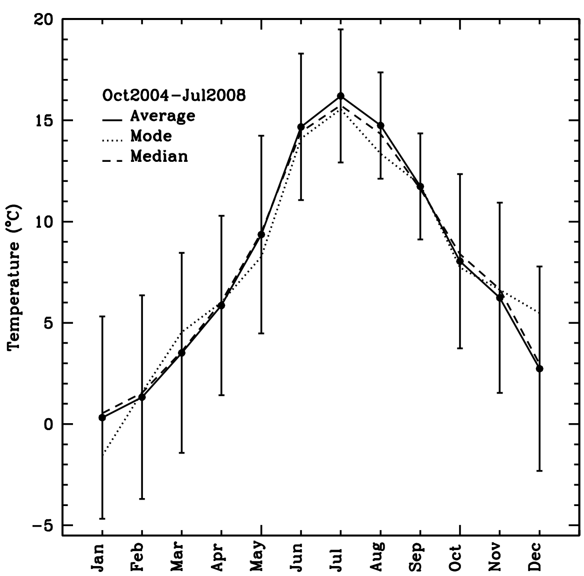

Fig. 1. Average, mode and median monthly temperature measured by the TMT weather station.

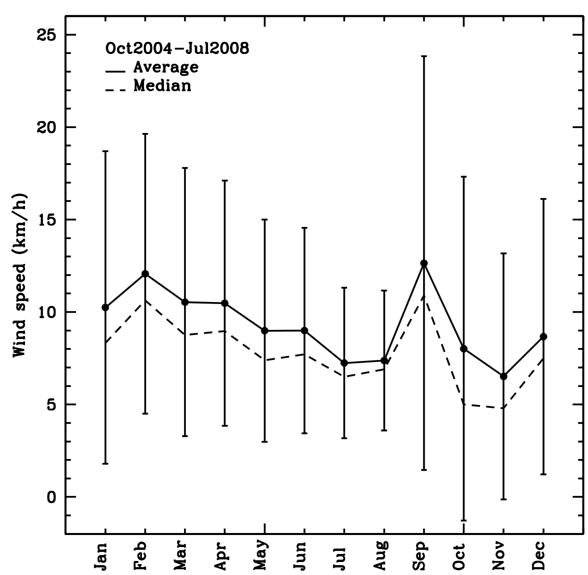

Fig. 2. Average and median monthly wind speed measured by the TMT weather station.

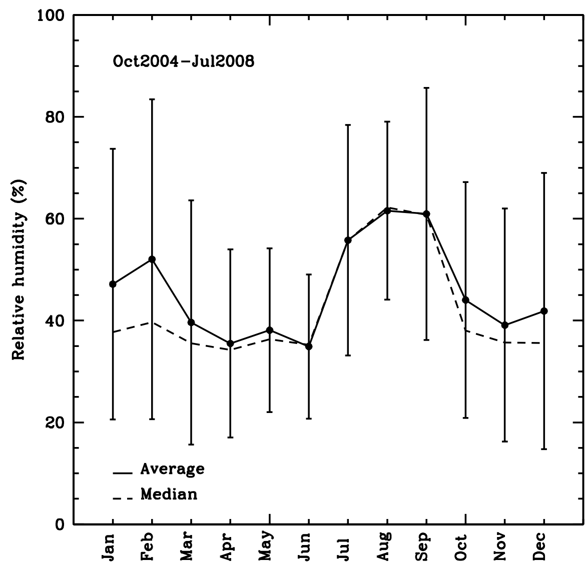

Fig. 3. Average and median monthly relative humidity measured by the TMT weather station.

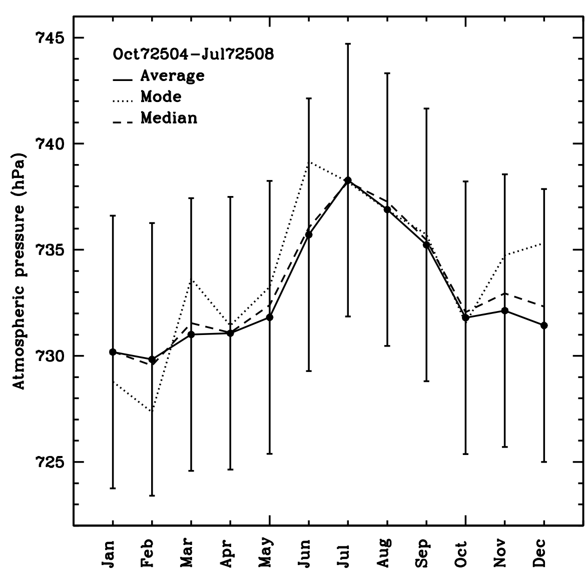

Fig. 4. Average, mode and median monthly pressure measured by the TMT weather station.

(no mode), relative humidity (no mode) and pressure are plotted in Figures 1, 2, 3 and 4. The following conclusions can be extracted from these data:

- Very dry conditions are found in April, May and June, when the relative humidity is less than $\sim$ 55% nearly 90% of the time.
- The wind speed tends to decrease between March and November and picks up during the winter months. The pronounced wind speed peak for September can not be assumed to be a typical monthly value, since weather data for this month could only be gathered during the 2006 season.

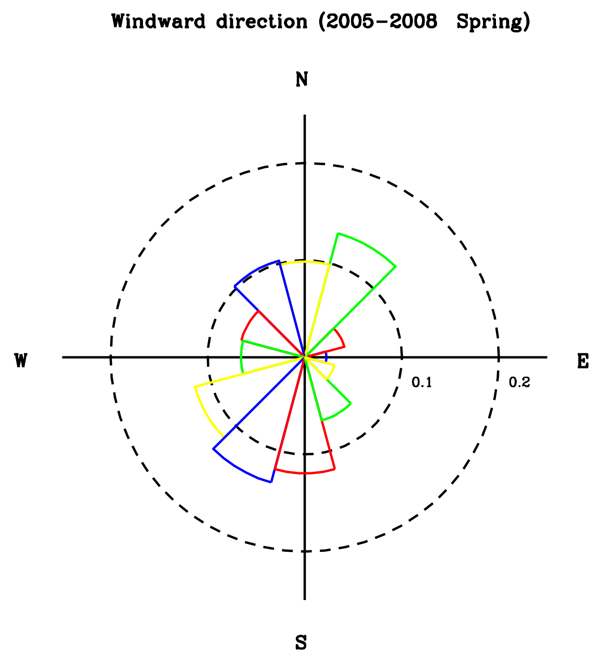

Fig. 5. Spring windward direction histogram. Each piece of pie is 30° wide.

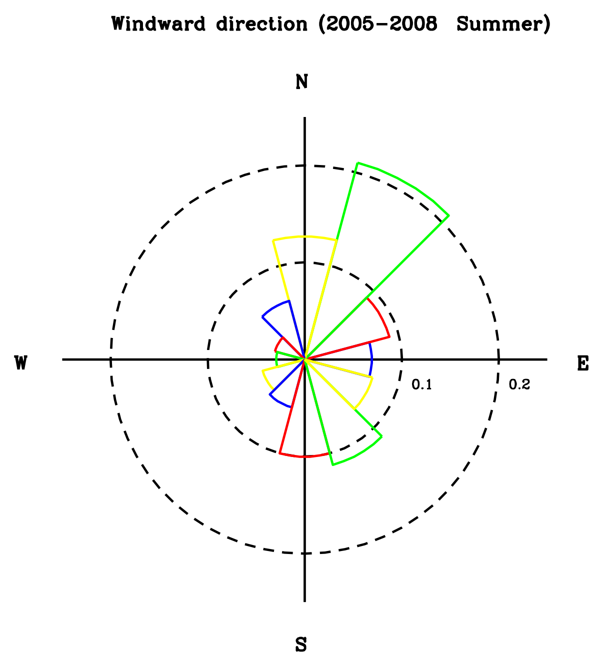

Fig. 6. Summer windward direction histogram. Each piece of pie is 30° wide.

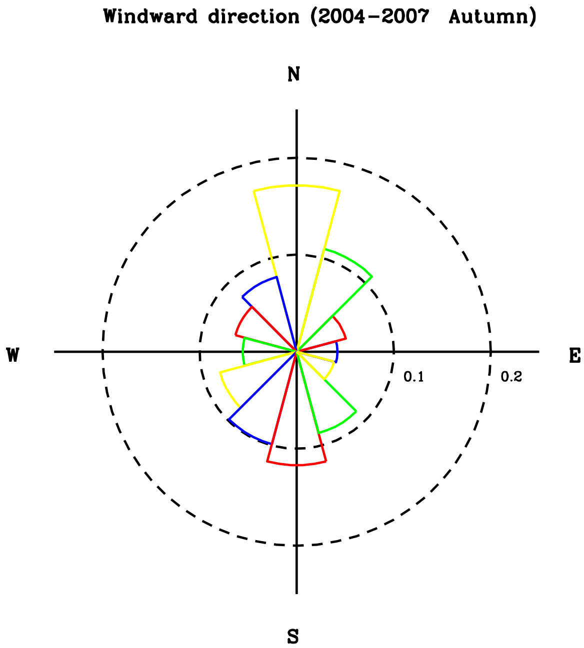

Fig. 7. Autumn windward direction histogram. Each piece of pie is 30° wide.

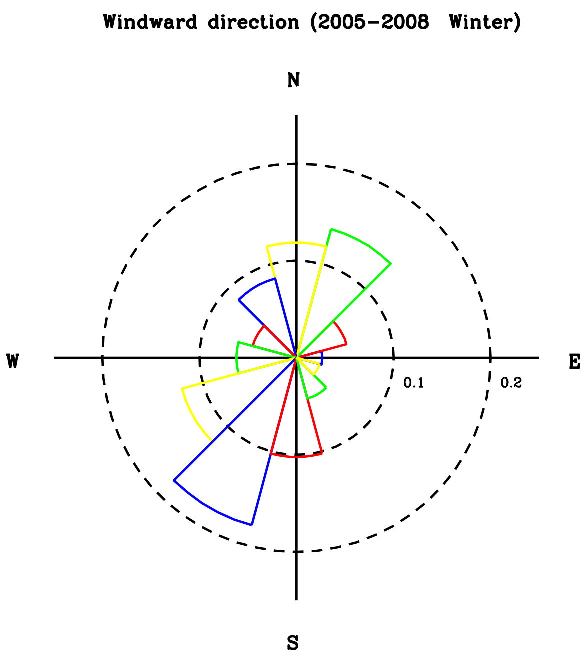

Fig. 8. Winter windward direction histogram. Each piece of pie is 30° wide.

- The monthly maximum and minimum average daily temperatures are 0.3°C (January) and 16.2°C (July), though variations larger than this can occur in a single month, as can be seen from Tables 4 and 5.

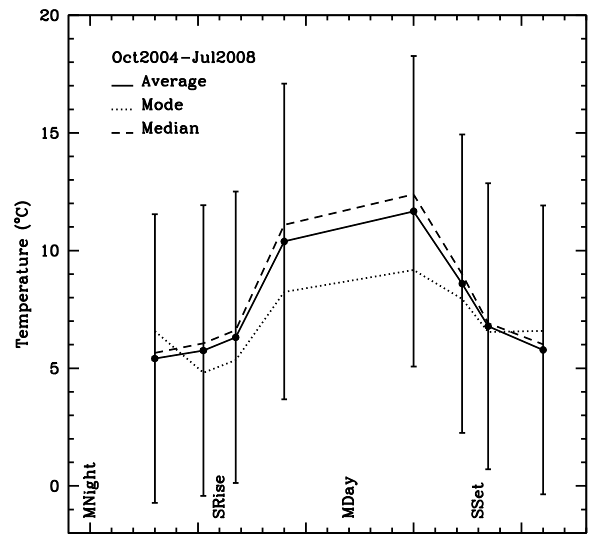

Fig. 9. Average, mode and median daily temperature measured by the TMT weather station.

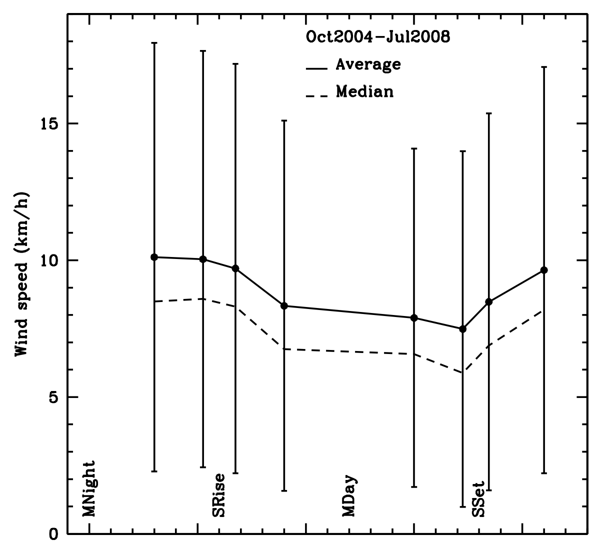

Fig. 10. Average and median daily wind speed measured by the TMT weather station.

Histograms for wind direction for spring, summer, autumn and winter are presented as pie charts in Figures 5, 6, 7 and 8. Given the variability of wind direction, we decided to construct these histograms using 30° intervals with all four cardinal directions centered. Notice that large intervals minimize the effect that nearby treetops could have had on wind direction. As can be seen from these figures, there is no overwhelmingly dominant wind direction in any season and the highest frequency is close to 0.21 (summer, northeasterly). Though there

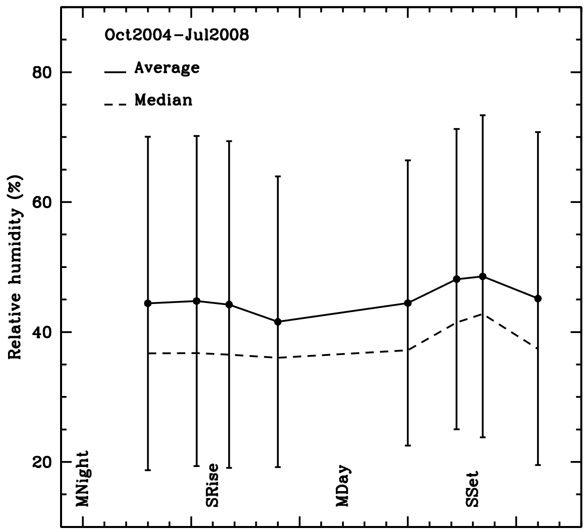

Fig. 11. Average and median daily relative humidity measured by the TMT weather station.

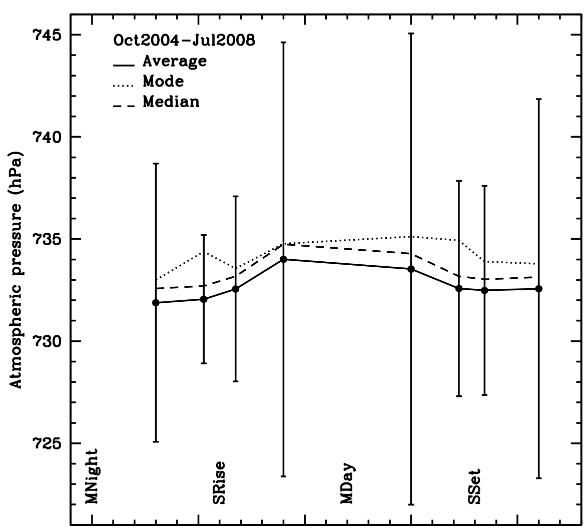

Fig. 12. Average, mode and median daily pressure measured by the TMT weather station.

are some seasonal differences, it is fair to say that the wind hardly ever blows from the northwest or from the southeast. The two predominant windward directions ($\sim \pm 30°$) are north and southwest during winter and spring, and north and south in summer and autumn. Wind power may have a different directional distribution, a point to be discussed in § 5.

The behavior of some weather variables as a function of wind direction provides interesting additional information on weather patterns at SPM. Wind flowing from the south and south-southeast is associated to warmer (up to ~ 4°C) and more humid (~ 10%

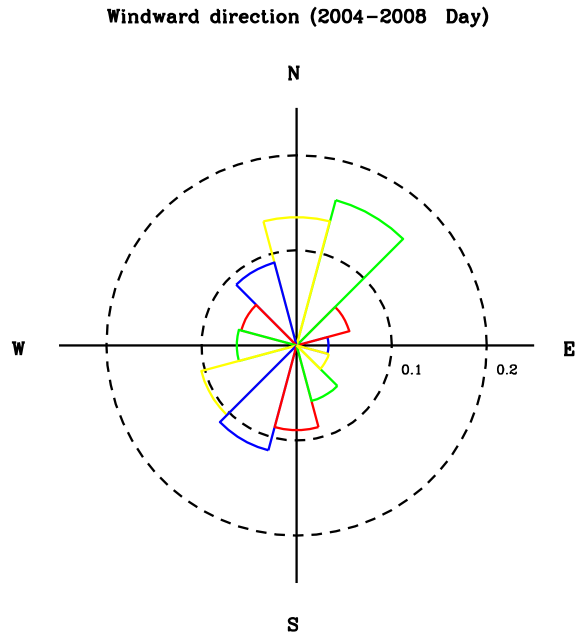

Fig. 13. Daytime (between sunrise and sunset) windward direction histogram. Each piece of pie is 30° wide.

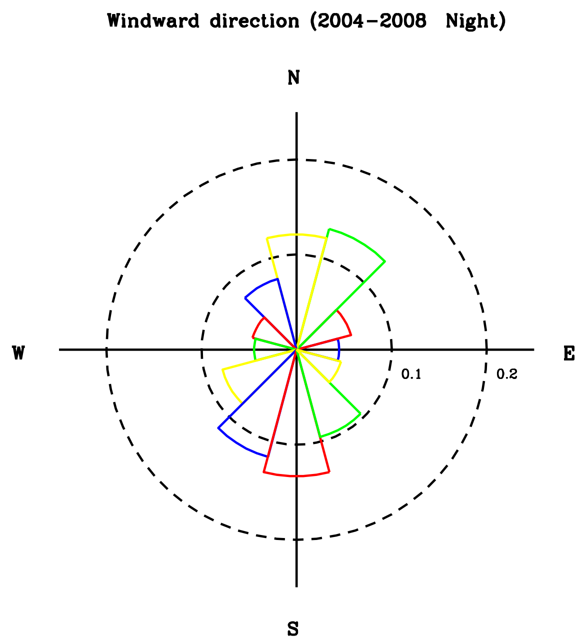

Fig. 14. Nighttime (between sunset and sunrise) windward direction histogram. Each piece of pie is 30° wide.

more) weather than wind blowing from the west and west-southwest. When there are easterly winds, the atmospheric pressure is somewhat larger (~ 4 hPa) and the average daily solar irradiation can be up to 170 W/m^2 smaller (more clouds, more humid weather).

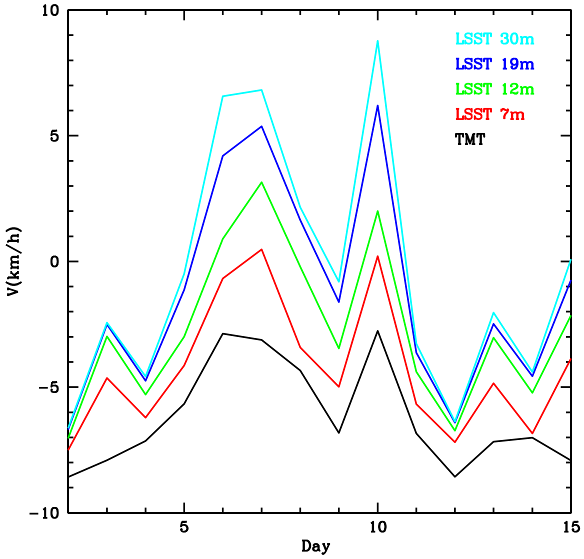

Fig. 15. Mean night wind speed measured by the TMT weather station and the ultrasonic anemometers of the LSST tower located 7, 12, 19 and 30 meters above ground level. The TMT site was located ∼ 10–15 higher than the LSST experiment, but the TMT anemometer was 2 meters above ground level.

Obviously, weather variables also change on a daily basis. We divided the day using 8 time periods: an hour and a half before and after sunrise (SR- and SR+) and sunset (SS- and SS+), and four equally long night (MN- and MN+) and daytime periods (MD- and MD+) around midnight and midday. Since the number of daytime hours is variable, the relative length of the night and daytime periods changes during the year (daytime lasts for 10.1 and 14.1 hours during the winter and summer solstices respectively). Statistics for a "typical" day between October 2004 and July 2008 are shown in Table 6, and average, mode and median daily values for temperature, wind speed, relative humidity (no mode), and pressure are plotted in Figures 9, 10, 11 and 12. We can draw the following conclusions from these data:

- Average temperature variations during the night and for the entire day are ∼ 2 and 6°C respectively.

- Wind speed is at its lowest point just before sunset, and is clearly larger (∼ 25%) during the night.

- Relative humidity is somewhat larger in the evening since summer rainstorms usually occur around this time of day.

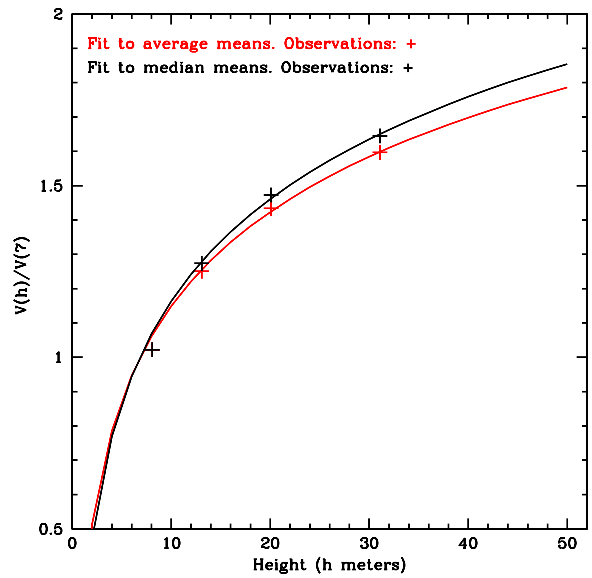

Fig. 16. Wind speed as a function of distance to ground level. Wind speeds are normalized with respect to their value at a 7 meter height. Continuous lines are fits to observations (plus signs), as given by Equation 1.

- There seems to be much less dispersion about the average atmospheric pressure during sunrise and sunset, but this may be produced by the smaller number of records that we have for these time windows (about a third compared to the midday and midnight time windows).

We also found that the shape of the mean and median daily variations of temperature, wind speed, pressure and, to a lesser extent, humidity, do not change drastically from month to month.

Histograms for wind direction for night (between sunset and sunrise) and day time (between sunrise and sunset) are presented as pie charts in Figures 13 and 14. As with the seasonal behavior, there is no overwhelmingly dominant windward direction and the wind hardly ever blows from the southeast or northwest. During the day, the predominant windward directions are north and southwest, but at night there is a slight shift and the wind flows mostly from north or south.

3. RESULTS FROM THE LSST ULTRASONIC ANEMOMETERS

The Large Synoptic Survey Telescope (LSST) site testing team installed four Metek Ultrasonic USA-1 anemometers on a tower standing some 45 meters to the NE from the site occupied by the TMT weather station. These anemometers were placed at a height of 7, 12, 19 and 30 meters above ground

TABLE 7

Height	V(h)/V(7)	Θ(h)- Θ(7)	Z(h)-Z(7)	T(h)-T(7)
	Means			
7	1.000	0.0	0.0	0.0
12	1.229±0.139	1.2±16.3	1.2±50.1	−0.17±0.13
19	1.412±0.234	1.4±41.3	1.4±38.9	−0.13±0.96
30	1.575±0.223	1.6±36.0	1.6±69.7	−0.41±0.71
	Medians			
7	1.000	0.0	0.0	0.0
12	1.252±0.175	1.3±43.4	1.3±47.1	−0.16±0.15
19	1.451±0.272	1.5±59.8	1.5±34.7	−0.13±1.02
30	1.623±0.294	1.6±49.0	1.6±60.3	−0.27±0.47

LSST weather station. Horizontal and vertical wind speed (V and Z), wind direction (Θ) and temperature (T) as a function of height h, relative to the value of these variables at a 7 m height, either as a ratio (horizontal wind speed) or a difference (the other variables).

level. Measuremens were conducted from December 15, 2005 to May 15, 2006, always between 18 and 6 hours local time (2 and 14 hours UT). The four stations were working simultaneously for only 60 days. The ultrasonic anemometers delivered the sound speed and three wind velocity components with a $\simeq$ 1 Hz sampling frequency. Assuming a dry atmosphere, the temperature is calculated from the speed of sound.

In Figure 15 we plot the mean daily horizontal wind speed measured by the TMT weather station, which was standing 2 m above ground level, and by the four ultrasonic anemometers for the aforementioned period of time. As can be seen, wind speed at TMT was always smaller than any value measured at LSST. This is not unexpected. Basic hydrodynamics predict larger wind speeds at higher altitudes.

In Table 2 we report average and median values of V(h)/V(7), Θ(h)- Θ(7), Z(h)-Z(7) and T(h)-T(7), where V, Θ, Z and T stand for the horizontal wind velocity, horizontal wind direction, the vertical wind speed and temperature, and h refers to the height at which the anemometer is (obviously, 7 stands for the ultrasonic anemometer located 7 meters above ground level). Statistics are for the mean and median values of these quantities for each of the 60 nights when the 4 ultrasonic anemometers at the LSST tower were working simultaneously. Temperature, wind direction and vertical wind speed were not expected to have a clear dependence on height above ground level at this scale, and none is observed (dispersions are much larger than averages for the mean and median values). On the other hand, as can be seen from Figure 16, the dependence of wind speed on height is very clear. A mean square fit to the standard relationship between these quantities,

$$V(h)/V(7) = K_1 + K_2 \ln(h/7)\,, \qquad (1)$$

yields $K_1 = 1.0077$ (1.0103) and $K_2 = 0.3960$ (0.4293). Constants out and in the parentheses are for fits to the mean average and median values respectively. The quality of this fit is evident from Figure 16. The roughness length, a parameter of some importance in surface layer research and in the wind power industry, is defined as the height where the wind speed is zero. From equation 1 we find a roughness length between 0.55 (average fit) and 0.67 (median fit) meters. This is typical of forests and very rough and uneven terrains, as it should be (e.g. Wallace & Hobbs 2006; `www.windpower.org`).

4. ENERGY CONSUMPTION AND CARBON FOOTPRINT OF THE SPM OBSEVATORY

Electric energy at the observatory is produced by diesel power plants. Diesel is also utilized to heat water for domestic use and air conditioning. The transportation fleet is made up of $\sim$ 30 vehicles, 25 taking in gasoline and the rest diesel. About two thirds of these vehicles are heavy duty trucks transporting fuel, water, provisions and personnel.

Between 2004 and 2007, diesel consumption at the observatory amounted to between 195 and 228 thousand liters a year, whereas total gasoline expenditures were between 16 and 24 thousand liters per year. In addition, some 50,000 liters of gasoline were bought each of these years in Ensenada, the operational base of the observatory. We can safely assume that 90% of the gasoline bought in Ensenada is for transportation to the observatory. Taking all these into account, considering the relative numbers of vehicles that use diesel, we estimate that roughly 5 thousand liters of diesel and 70,000 liters of gasoline were spent every year between 2004 and 2007 to keep in motion the transportation fleet supporting the observatory. About 210 thousand liters of diesel were used for electric power generation and water heating.

The emission factors of greenhouse gases (hereafter GHG) produced by the combustion of diesel and gasoline in Ensenada between 2004 and 2007 were close to 2.4 and 2.7 kg(CO_2^{eq})/l respectively, where CO_2^{eq} includes the three major GHG except water vapor: carbon dioxide, methane and nitrous oxides (Bohigas 2009, in preparation). These numbers are intermediate between those used in Mexico and the U.S., since a large amount of the fuel sold in Baja California is imported.

From the preceding emission factors and volumes of diesel and gasoline, we conclude that GHG emission due to transportation and energy generation of the SPM observatory between 2004 and 2007 was close to 749 tons of CO_2^{eq} a year, or 2050 kg(CO_2^{eq})/day. It is likely that this volume has not changed much during the past 20 years, since the operation of the observatory has hardly been modified during this period. Some 1500 l of LPG a year are also spent in SPM. Since the emission factor of LPG is 1.53 kg(CO_2)/l (Bohigas 2009, in preparation), its combustion adds another 2.3 tons a year to the carbon footprint of SPM. Other day-to-day emissions, such as those resulting from waste disposal or airplane transportation for observers, are more difficult to quantify. In conclusion, the carbon footprint of the SPM observatory under normal circumstances is probably somewhat more than 750 tons of CO_2^{eq} a year, but it may have been substantially larger when there were important construction activities going on.

If our preceding assumptions are correct, transportation produced 182 tons of CO_2^{eq} a year, or 497 kg(CO_2^{eq})/day. Taking into account the number of vehicles used by the SPM observatory, we conclude that the mean GHG emission produced by each vehicle in the SPM fleet is close to 17 kg(CO_2^{eq})/day. The mean GHG emission produced by vehicles in Ensenada between 2004 and 2007 was 15.3 kg(CO_2^{eq})/day, slightly less than in the observatory (Bohigas 2009, in preparation). The difference is probably associated to the larger fraction of heavy duty vehicles used by the SPM operation, which will increase the carbon footprint, better maintenance for these vehicles, which has the opposite effect, as well as important uncertainties in the input data.

Diesel combustion for energy generation emits 567 tons of CO_2^{eq} a year, 1552 kg($CO_2^e q$)/day. Discounting emissions produced by water heating, the use of electricity at OAN discharged $\simeq$ 500 tons of CO_2^{eq} a year, or 1370 kg($CO_2^e q$)/day. During the same period of time, electric expenditure per household, commercial and agricultural establishment and mid-scale industry in Ensenada gave off an average of 4, 12, 159 and 450 kg(CO_2^{eq})/day respectively, whereas big industries generated close to 60 tons of CO_2^{eq} a day (Bohigas 2009, in preparation). Within a factor of 2, the same numbers are found for Baja California and Mexico. Thus, the generation of electricity at the observatory is emitting 3 times more GHG than a typical mid-scale industry and almost 10 times more than the average agricultural establishment in the region.

The preceding comparison suggests that energy use and/or generation may be inefficient. Peak electric energy consumption at the observatory is close to 48 KWh, which implies that 1.2 kg of CO_2^{eq} are emitted per kWh. On the other hand, the consumption of 1 kWh in Mexico, Baja California and Ensenada leads to the emission of 0.78, 0.57 and 0.85 kg of CO_2^{eq}. Quite clearly, electric energy production at SPM is much more inefficient. This is not surprising, since there is a huge difference between a modern electric power plant and a commercial diesel combustion engine. In addition, natural gas is becoming the dominant fuel for the electric industry in Mexico and Baja California. In terms of GHG emissions, a direct connection to the electric power grid would seem advisable, were it not for the damages and dangers that the construction and operation of power lines would and could do to the national park. Furthermore, as we shall see in the following section, renewable energies are an available option to modernize electric power generation, as well as to protect the fragile ecological environment and reduce GHG emissions.

Renewable energies can also be used for transportation if the present fleet is substituted by one based on electric cars. Using data from the Secretaría de Energía in Mexico and the Department of Energy in the U.S., we find that the mean energy density of gasoline and diesel in these countries between 2004 and 2007 was roughly equal to 33.3 and 37 $\times 10^6$ J/l. Taking into account the amount of fuel used at the observatory for transportation, we estimate that 9.6 $\times 10^7$ J, or 27 kWh, were required to keep it going for an hour. Thus, all things being equal, the existence of a transport fleet based on electric cars is conditioned by the existence of a source capable of delivering this amount of energy. Finally, $\sim$ 30 kWh are required to heat water at peak demand. Adding all things up, the peak energy demand of the Observatory is close to 110 kWh.

A final point of interest stands out when the electricity bill is considered. No more than 7% of the electric energy supply, or 3 out of 48 kWh, is taken up by the telescopes, which suggests that resources are probably not being properly used. It is a known fact that established institutions tend to grow beyond their needs. The huge difference between the energy used to run telescopes and support, suggests that this may be the case at SPM.

5. THE POTENTIAL OF RENEWABLE ENERGIES

Statistics for the entire TMT campaign for daytime solar irradiation, P_r, humid air density, ρ, and wind power density 50 meters above ground level, P_{50}, are presented in Table 8. Daytime solar irradiation is given for data set VT and between sunrise and sunset, a period of time somewhat longer than the one used to define sunshine duration, which applies to solar irradiation exceeding $\sim$ 120 W/m^2. Humid air density and wind power are given for data set V0, which excludes all registers where the anemometer was obviously not working. Humid air density is found from

$$\rho = P_d/(R_d T) + P_v/(R_v T)\,, \tag{2}$$

where R_d and R_v are the dry air and vapor gas constants (287.05 and 461.495 Joules/kg K respectively) and P_d and P_v are the dry air and water vapor pressures. The water vapor pressure is $P_v = E_s\,H$, where E_s is the water vapor saturation pressure over liquid water and H is the relative humidity. Water vapor saturation pressure can be determined using Bolton's (1980) equation 10, which we found to be better than 0.5% accurate within our observed temperature range. Wind power 2 meters above ground, given by $\rho \mathrm{V}^3/2$, was determined every time we had a valid register and was scaled with equation (1) in order to obtain P_{50}.

As can be seen from Table 8, there is much more power available from daytime solar irradiance than from wind. There was no measurable wind at least 12.5% of the time, and wind gusts were rare but exceptionally intense. But wind power can have as much energy as daytime solar irradiation $\sim$ 10% of the time, and is the only renewable energy source at night.

TABLE 8

	ρ	P_{50}	P_r
Max	0.969	3.0×10^5	1384.2
Min	0.844	0.0	0.0
Average	0.908	498.2	503.5
σ	0.015	1960.9	330.4
Mode	0.902	0.0	35.5
O1	0.888	0.0	78.3
Q1	0.895	9.4	191.8
O3	0.901	28.3	334.4
Median	0.907	65.9	492.0
O5	0.914	141.3	646.9
Q3	0.921	320.2	786.5
O7	0.930	828.8	944.1

Wind and daytime solar energy flux. Statistics for wind density (ρ, in kg/m^3), wind power 50 meter above ground level (P_{50}, in W/m^2) and daytime solar irradiation (P_r, in W/m^2) between October 2004 and July 2008. Symbols O1, O3, O5 and O7 stand for the first, third, fifth and seventh octiles of the distribution, whereas Q1 and Q3 stand for the first and third quartile.

Wind turbines are designed to start running at wind speeds around 15 km/h, the cut-in wind speed, and are shut down when the average wind speed after a certain amount of time (5 to 10 minutes) exceeds the cut-off speed at $\simeq$ 90 km/h (see `www.windpower.org` and `www.awea.org`). Thus, wind farming is only possible when wind speed is consistently within these two numbers. In order to estimate the amount of time available for productive wind harvesting we use the following scheme:

- Class 1: $\mathrm{V} < 15$
- Class 2: $15 \leq \mathrm{V} < 60$
- Class 3: $60 \leq \mathrm{V} < 90$
- Class 4: $90 \leq \mathrm{V}$,

where wind speed V is in km/h. Assuming that turbines respond instantaneously to any change in wind speed, eolic energy can not be harvested in Class 1 (herein C1) and Class 4 (herein C4) winds, but farming is viable for Class 2 and Class 3 winds. In our case, instantaneous is understood as the time taken to register a new weather record, i.e. roughly

TABLE 9

	ρ	P_{50}	P_r	ρ	P_{50}	P_r	ρ	P_{50}	P_r
	Jan			Feb			Mar		
Max	0.969	9.5×10^4	1076.5	0.965	5.6×10^4	1195.1	0.957	3.0×10^5	1247.3
Min	0.894	0.0	19.2	0.886	0.0	26.3	0.884	0.0	26.3
Average	0.930	784.6	410.6	0.926	807.1	459.4	0.920	648.9	540.3
σ	0.013	2627.8	234.2	0.014	1844.7	279.9	0.016	2553.5	331.5
Mode	0.923	0.0	697.0	0.926	0.0	34.5	0.921	0.0	962.9
O1	0.916	0.0	96.6	0.909	15.8	98.7	0.905	9.4	82.7
Q1	0.922	14.9	199.6	0.916	51.1	199.6	0.911	28.3	212.4
O3	0.925	44.6	308.2	0.921	112.7	318.5	0.916	56.5	386.1
Median	0.929	107.1	423.2	0.925	221.8	451.9	0.920	122.4	572.0
O5	0.934	238.0	528.0	0.930	410.2	590.6	0.924	235.5	743.5
Q3	0.938	529.5	622.2	0.936	748.2	723.1	0.929	489.8	865.3
O7	0.946	1404.1	703.3	0.943	1626.7	819.1	0.936	1158.5	937.6
C1		0.337			0.195			0.271	
C2		0.580			0.712			0.664	
C3		0.064			0.078			0.053	
C4		0.019			0.015			0.012	
	Apr			May			Jun		
Max	0.959	5.3×10^4	1217.6	0.944	4.8×10^4	1328.9	0.917	2.7×10^4	1346.1
Min	0.881	0.0	25.0	0.864	0.0	13.8	0.861	0.0	10.2
Average	0.913	531.4	584.7	0.903	378.5	605.7	0.891	327.1	561.2
σ	0.013	1229.2	374.9	0.016	1138.4	376.3	0.006	847.6	374.9
Mode	0.911	0.0	1047.2	0.907	1.5	1065.8	0.893	0.9	1051.8
O1	0.898	9.9	69.7	0.888	7.5	74.0	0.879	8.6	60.9
Q1	0.905	29.8	187.5	0.894	19.4	216.9	0.883	22.3	168.0
O3	0.909	64.5	406.8	0.899	38.8	448.7	0.888	45.4	371.1
Median	0.913	130.7	636.2	0.903	71.7	674.2	0.892	81.4	577.6
O5	0.917	248.2	832.9	0.907	134.4	853.9	0.894	144.9	785.6
Q3	0.921	493.1	959.8	0.911	274.7	974.5	0.897	269.2	939.6
O7	0.927	1143.4	1029.9	0.917	691.3	1045.5	0.901	607.0	1029.0
C1		0.262			0.337			0.308	
C2		0.681			0.627			0.661	
C3		0.051			0.032			0.028	
C4		0.006			0.004			0.003	

Typical month statistics for air density (ρ in kg/m^3), wind power 50 meters above ground level (P_{50} in W/m^2) and solar irradiance (P_r in W/m^2) for January, February, March, April, May and June, between October 2004 and July 2008. Symbols O1, O3, O5 and O7 stand for the first, third, fifth and seventh octiles of the distribution, whereas Q1 and Q3 stand for the first and third quartile. C1, C2, C3 and C4 are the fraction of registers where wind velocity can be classified as Class 1, 2, 3 or 4 respectively (see § 5).

2 minutes. The separation of low (Class 2, herein C2) and high (Class 3, herein C3) power winds at 60 km/h is arbitrary, though sizable wind turbines work at peak efficiency close to this velocity. Using this scheme we find the following fractions for each wind class between October 2004 and July 2008: 0.37 for C1, 0.58 for C2, 0.04 for C3 and 0.01 for C4. Thus, this simple analysis implies that wind in SPM can be harvested $\sim 60\%$ of the time.

As we saw in § 2, wind conditions change appreciably during the day and throughout the year. Typical month and day statistics for solar irradiation (using set VT), air density and wind power 50 meter above ground (using set V0), as well as fractions for each one of the wind classes defined above, can be found in Tables 9, 10 and 11. For daily statistics we use the 8 time periods defined in § 2. A clear picture of wind availability can be obtained from Figures 17

TABLE 10

	ρ	P_{50}	P_r	ρ	P_{50}	P_r	ρ	P_{50}	P_r
	Jul			Aug			Sep		
Max	0.909	1.2×10^4	1366.9	0.910	1.2×10^4	1369.9	0.919	9.6×10^4	1384.2
Min	0.861	0.0	0.0	0.844	0.0	0.0	0.878	0.0	9.2
Average	0.889	148.7	472.8	0.892	137.3	500.6	0.900	1476.2	488.3
σ	0.008	368.7	356.0	nan	263.4	339.3	0.004	3841.0	317.1
Mode	0.894	0.0	44.9	0.895	0.0	0.0	0.905	0.0	30.3
O1	0.877	5.4	61.3	0.883	6.6	93.3	0.889	0.0	105.2
Q1	0.883	14.3	141.4	0.887	17.8	192.0	0.894	6.0	215.0
O3	0.887	27.9	257.2	0.890	35.3	298.4	0.898	66.0	313.4
Median	0.890	48.8	392.6	0.894	58.6	4 44.9	0.901	231.1	430.2
O5	0.893	81.6	570.2	0.896	94.2	631.7	0.904	585.2	601.8
Q3	0.896	141.6	810.5	0.898	152.0	831.8	0.905	1284.5	787.2
O7	0.900	283.2	988.1	0.901	282.7	967.7	0.908	3019.1	920.1
C1		0.406			0.357			0.321	
C2		0.583			0.640			0.505	
C3		0.006			0.002			0.126	
C4		0.005			0.001			0.048	
	Oct			Nov			Dec		
Max	0.944	2.3×10^5	1217.9	0.962	3.9×10^4	959.1	0.960	4.9×10^4	962.8
Min	0.876	0.0	11.0	0.867	0.0	13.0	0.883	0.0	0.0
Average	0.907	781.9	503.9	0.913	285.0	429.1	0.924	481.3	375.7
σ	0.016	3745.1	287.8	0.017	948.3	243.2	0.011	1435.8	220.4
Mode	0.908	0.0	35.5	0.914	0.0	34.0	0.920	0.0	29.6
O1	0.894	0.0	101.8	0.900	0.0	97.4	0.909	0.0	73.4
Q1	0.900	0.0	236.1	0.905	0.0	208.3	0.916	4.6	174.6
O3	0.903	0.0	384.2	0.909	3.6	324.2	0.920	26.1	278.3
Median	0.907	21.2	543.5	0.913	19.3	449.6	0.924	76.8	392.7
O5	0.910	77.7	676.5	0.917	61.6	563.7	0.928	173.5	490.1
Q3	0.914	282.5	776.7	0.921	181.0	655.7	0.932	365.4	573.8
O7	0.919	1031.2	842.0	0.927	548.0	726.5	0.938	899.7	651.7
C1		0.535			0.552			0.395	
C2		0.392			0.420			0.554	
C3		0.050			0.025			0.043	
C4		0.023			0.003			0.008	

Typical month statistics for air density (ρ in kg/m^3), wind power 50 meters above ground level (P_{50} in W/m^2) and solar irradiance (P_r in W/m^2) for July, August, September, October, November and December, between October 2004 and July 2008. Symbols O1, O3, O5 and O7 stand for the first, third, fifth and seventh octiles of the distribution, whereas Q1 and Q3 stand for the first and third quartile. C1, C2, C3 and C4 are the fraction of registers where wind velocity can be classified as Class 1, 2, 3 or 4 respectively (see § 5).

and 18, where the yearly and daily evolution of the wind class fractions are plotted. From these figures and tables we can conclude the following:

- Conditions are particularly favorable in February, when wind can be harvested $\sim$ 80% of the time and the median wind power density is large. Wind energy availability decreases consistently between March and October, and picks up between November and February. Winter and spring are the best seasons, whereas autumn is comparatively poor. The least propitious month is October, when wind can be utilized $\sim$ 45% of the time and the median power density is roughly 10 times less than in February.

- On a daily basis, conditions to extract wind energy improve steadily during the night, and just before sunrise wind can be harvested close to 69% of the time. The amount of time that wind can be used to produce electric power decreases

TABLE 11

	ρ	P_{50}	P_r	ρ	P_{50}	P_r	ρ	P_{50}	P_r	ρ	P_{50}	P_r
	SR-			SR+			MD-			MD+		
Max	0.969	9.6×10^4	250.7	0.969	1.3×10^5	556.4	0.967	2.3×10^5	1369.9	0.960	3.0×10^5	1384.2
Min	0.858	0.0	0.0	0.853	0.0	0.0	0.847	0.0	33.4	0.851	0.0	27.8
Average	0.914	635.7	19.1	0.913	593.5	116.9	0.902	431.2	614.5	0.897	339.4	640.3
σ	0.018	2246.7	16.5	0.017	2235.5	83.6	0.015	2117.1	291.6	0.015	1660.0	273.6
Mode	0.902	0.0	0.0	0.900	0.0	35.5	0.890	0.0	1065.8	0.894	0.0	1051.8
O1	0.896	3.0	1.1	0.895	0.0	35.1	0.883	0.0	224.9	0.879	0.0	294.5
Q1	0.902	21.0	7.6	0.900	15.8	45.9	0.889	7.1	391.5	0.885	9.4	422.2
O3	0.907	54.0	14.6	0.906	47.5	62.7	0.894	21.2	516.6	0.890	18.8	542.3
Median	0.914	114.0	21.3	0.912	102.8	91.1	0.900	49.4	630.5	0.895	47.1	659.3
O5	0.919	216.1	26.2	0.918	197.8	127.4	0.906	105.9	740.4	0.901	94.2	754.8
Q3	0.926	450.2	27.4	0.925	403.5	173.1	0.913	233.1	860.4	0.907	188.4	866.6
O7	0.934	1104.4	29.4	0.933	1012.6	228.4	0.923	635.7	980.2	0.918	499.2	987.9
C1		0.297			0.317			0.407			0.417	
C2		0.640			0.626			0.554			0.552	
C3		0.050			0.046			0.031			0.025	
C4		0.013			0.011			0.008			0.006	
	SS-			SS+			MN-			MN+		
Max	0.963	1.8×10^5	531.7	0.961	8.9×10^4	61.3	0.969	7.1×10^4	35.8	0.967	1.6×10^5	35.3
Min	0.848	0.0	0.0	0.844	0.0	0.0	0.848	0.0	0.0	0.862	0.0	0.0
Average	0.912	430.5	131.8	0.906	351.3	17.0	0.915	560.0	16.7	0.915	666.6	17.2
σ	0.018	1675.4	90.1	0.016	1667.7	11.0	0.017	1650.9	10.8	0.017	2302.2	10.8
Mode	0.901	0.0	34.8	0.897	0.0	0.0	0.903	0.0	0.0	0.914	0.0	0.0
O1	0.894	0.0	38.6	0.888	0.0	0.5	0.896	0.0	0.3	0.897	0.0	0.8
Q1	0.899	5.5	54.7	0.893	5.6	6.3	0.903	15.6	6.4	0.903	14.9	7.2
O3	0.905	22.2	77.3	0.899	13.9	12.9	0.908	44.6	12.5	0.909	49.7	13.3
Median	0.911	55.4	105.8	0.904	36.1	19.5	0.915	98.2	19.3	0.915	109.3	19.8
O5	0.916	127.5	143.3	0.910	77.9	25.1	0.920	205.3	24.6	0.920	228.6	25.6
Q3	0.923	288.2	195.1	0.917	178.0	26.9	0.926	428.4	26.7	0.926	482.1	26.9
O7	0.930	759.3	258.9	0.925	539.4	28.5	0.934	1044.3	28.3	0.934	1197.9	28.5
C1		0.412			0.482			0.332			0.310	
C2		0.546			0.484			0.608			0.620	
C3		0.036			0.028			0.050			0.057	
C4		0.006			0.006			0.010			0.013	

Typical day statistics for air density (ρ in kg/m^3), wind power 50 meters above ground level (P_{50} in W/m^2) and solar irradiance (P_r in W/m^2). Symbols O1, O3, O5 and O7 stand for the first, third, fifth and seventh octiles of the distribution, whereas Q1 and Q3 stand for the first and third quartile. SR- and SR+ extend for 1.5 hours before and after sunrise, SS- and SS+ extend for 1.5 hours before and after sunset, MD- and MD+ are the first and second part of the day (equally divided) and MN- and MN+ are before and after midnight (also equally divided). C1, C2, C3 and C4 are the percentage of registers where wind velocity can be classified as Class 1, 2, 3 or 4 respectively (see §5).

during the day, with a minimum of $\sim$ 50% just after sunset, when the wind power density is almost 4 times smaller than at dawn (114 *vs.* 36 W/m^2)

The power contained in Class 2 and Class 3 winds is a rough estimate of the amount of eolic energy that can be used to produce electricity at SPM. In Figures 19 and 20 we present the monthly and daily variation of available wind and solar irradiation power, as well as the sum of these two quantities. Notwithstanding September, for which we have insufficient information, it is obvious that the median wind energy decreases as the year goes by, picking up rather dramatically in October, an unexpected irregularity that needs to be confirmed. Thus, wind energy is more readily available and more energetic in the winter months. Solar irradiation is more plentiful in spring, when skies are clear and humidity is at its lowest point. Summer days are longer, but skies are more often covered with clouds. As far as daily behavior is concerned, it is fortunate that weak winds

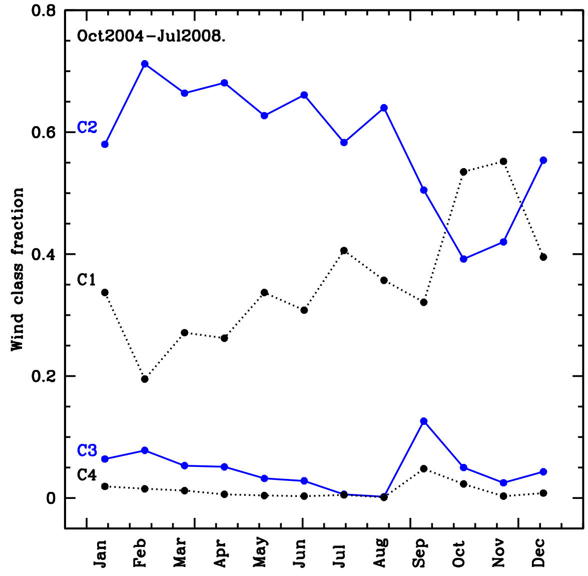

Fig. 17. Monthly variation of the fraction of time where wind speed could be classified as Class 1, 2, 3 and 4 (C1, C2, C3 and C4 respectively). The wind velocity in Class 1 winds is not sufficient to get the wind turbine going (i.e. it is less than the cut-in speed), and in Class 4 winds it is above the safety limit (i.e. larger han the cut-off speed). The addition of Class 2 and Class 3 wind is the fraction of time when wind can be harvested, with C3 standing for higher energy winds.

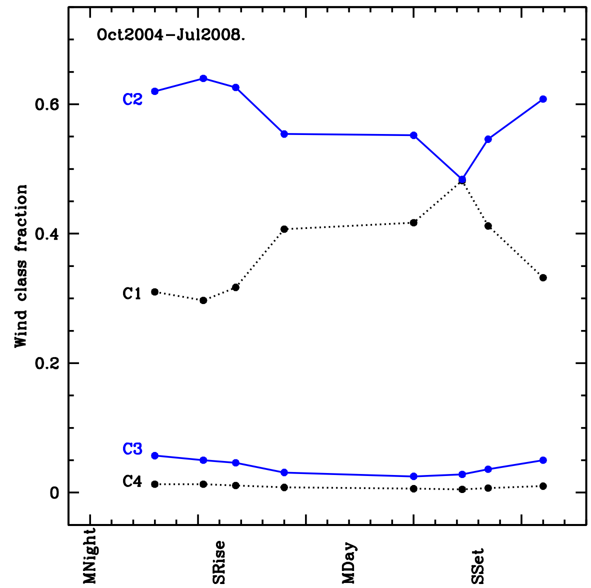

Fig. 18. Daily variation of the fraction of time where wind speed could be classified as Class 1, 2, 3 and 4 (C1, C2, C3 and C4 respectively). The wind velocity in Class 1 winds is not sufficient to get the wind turbine going (i.e. it is less than the cut-in speed), and in Class 4 winds it is above the safety limit (i.e. larger han the cut-off speed). The addition of Class 2 and Class 3 wind is the fraction of time when wind can be harvested, with C3 standing for higher energy winds.

are more frequent at daytime, when solar irradiance is plentiful. In conclusion, radiant and wind energy combined are more available and potent during the winter months, when they are more needed, and should provide sufficient power throughout most days and nights.

The relative amount of wind power $\wp(j)$ flowing from direction j during any time interval can be defined as,

$$\wp(j) = \frac{\mathrm{P}_{50}(j)\mathrm{n}(j)}{\sum_i \mathrm{P}_{50}(i)\mathrm{n}(i)}\,, \qquad (3)$$

where $\mathrm{P}_{50}(i \,\mathrm{or}\, j)$ is the median wind power flowing 50 meters above ground level from direction i or j, and $\mathrm{n}(i$ or $j)$ is the number of times that wind has been flowing from this direction during the prescribed period of time. In Figures 21, 22, 23 and 24 we plot the directional distribution of the relative amount of useful wind power, i.e. wind classes C2 and C3, during spring, summer, autumn and winter. As can be seen, $\sim$ 55 to 70% of useful wind power flows from the south and south-southwest, and $\sim$ 20 to 25% from the north and north-northeast with very small shifts from season to season. Not unexpectedly, the same pattern is observed throughout any typical day

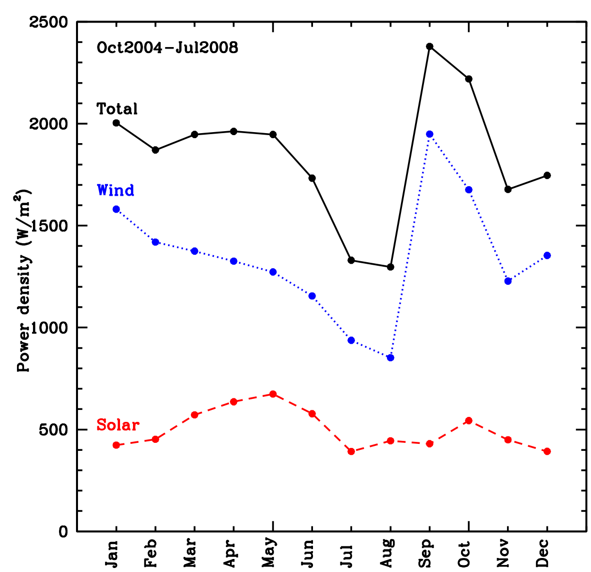

Fig. 19. Daily energy supply of radiant and wind energy when both are available.

(see Figures 25 and 26). This implies that wind turbines must be aligned along a NW-SE axis to avoid turbulence spillover, a specification that is specially

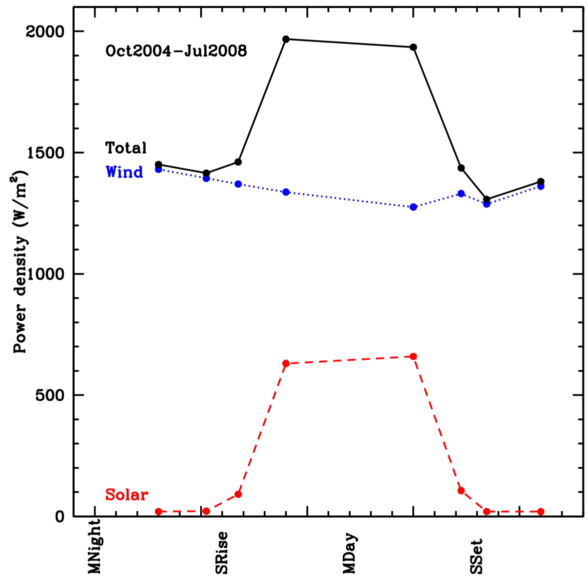

Fig. 20. Daily energy supply of radiant and wind energy when both are available.

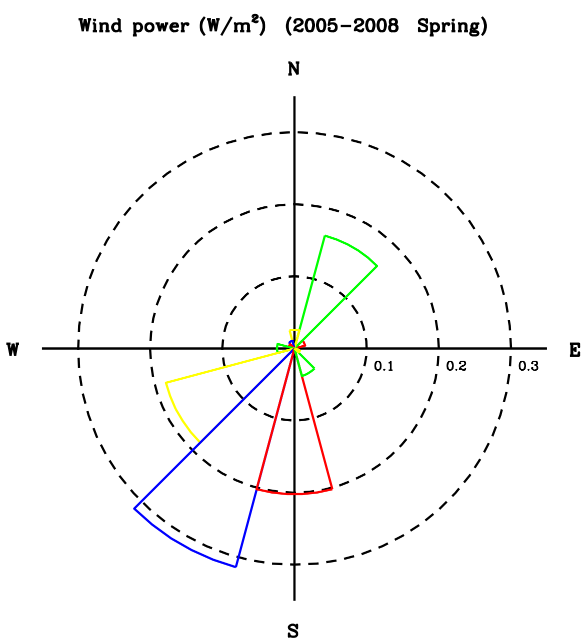

Fig. 21. Relative amount of wind power, $\wp(j)$ as defined in equation 3, flowing from direction j during spring.

relevant regarding telescopes. Since OAN telescopes are aligned along this axis, conflicts would be minor if a wind farm with two or more towers were to be installed.

Take notice that not all of this energy can be extracted. For instance, the production of electricity from solar energy depends on the efficiency of

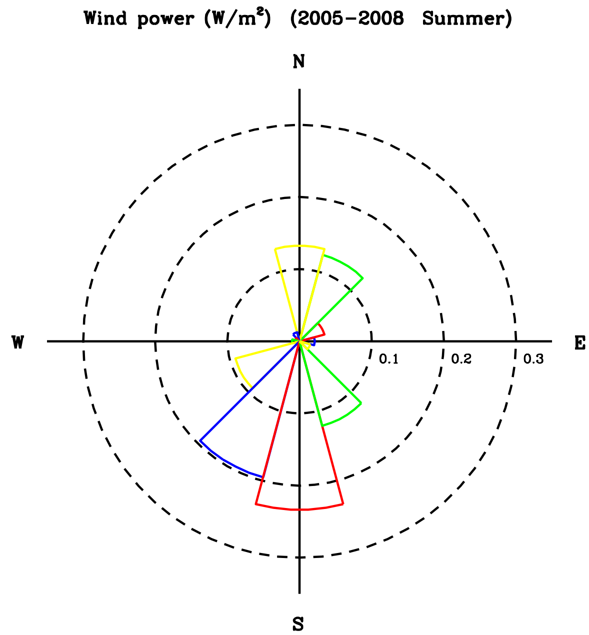

Fig. 22. Relative amount of wind power, $\wp(j)$ as defined in equation 3, flowing from direction j during summer.

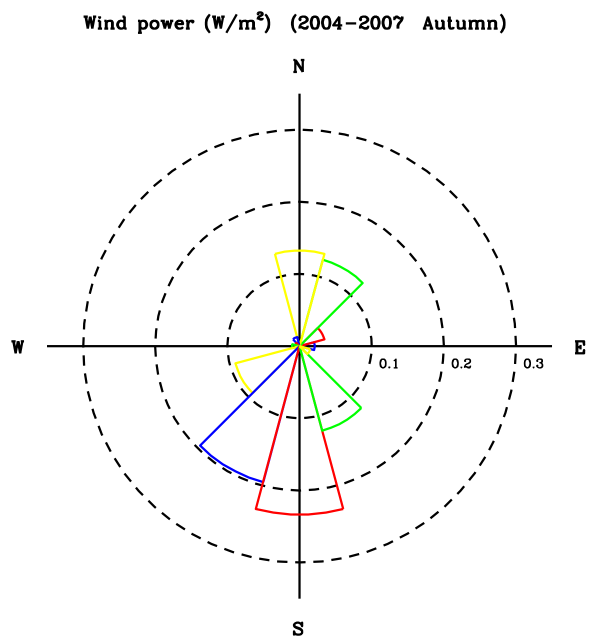

Fig. 23. Relative amount of wind power, $\wp(j)$ as defined in equation 3, flowing from direction j during autumn.

photovoltaic cells, nowadays close to 20%. Thus, roughly 5000 m^2 of photovoltaic cells are required to produce at all times between sunrise and sunset the 110 kWh that are currently being used at the observatory. Similarly, a rather large gathering area is

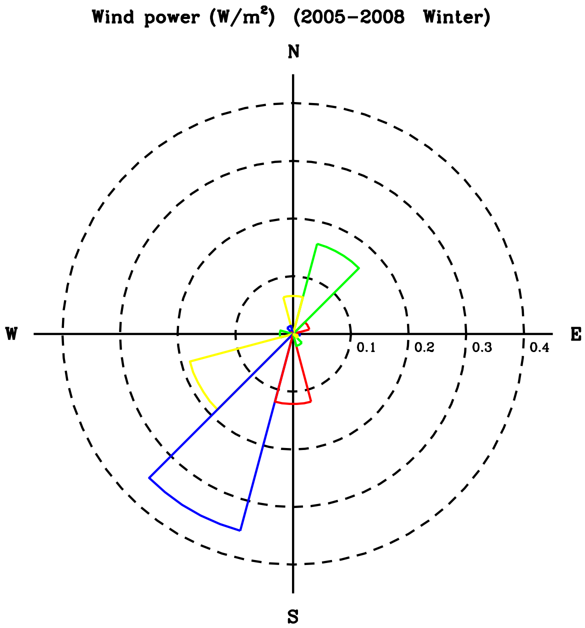

Fig. 24. Relative amount of wind power, $\wp(j)$ as defined in equation 3, flowing from direction j during winter.

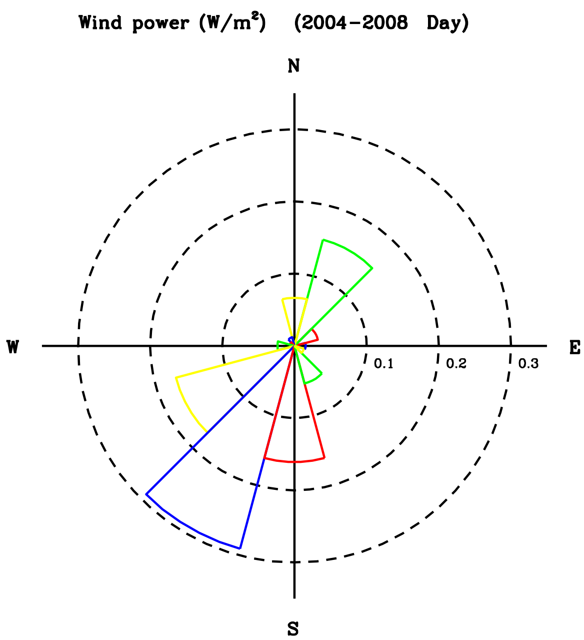

Fig. 25. Relative amount of wind power, $\wp(j)$ as defined in equation 3, flowing from direction j during daytime.

needed if solar energy is used to heat a liquid and/or produce water vapor to move a turbine and generate electricity. On the other hand, in addition to technical limitations, the extraction of wind energy is constrained by Betz' law, which establishes that

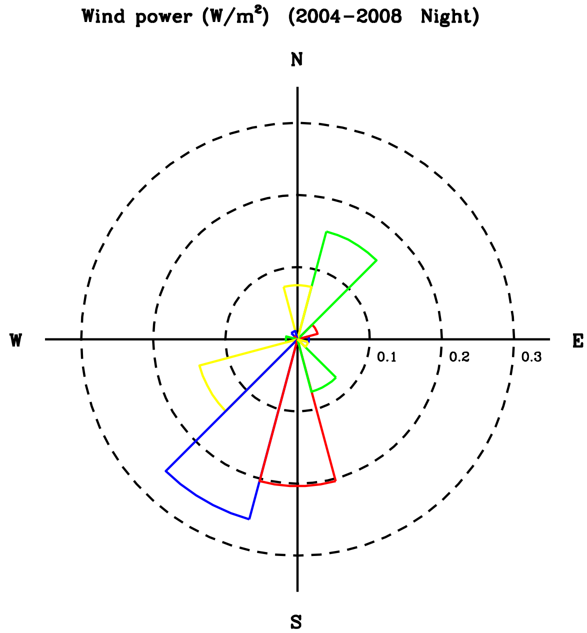

Fig. 26. Relative amount of wind power, $\wp(j)$ as defined in equation 3, flowing from direction j during nighttime.

no more than 16/27 (or 59%) of the wind kinetic energy can be used. Additionally, devices to store energy that is not immediately spent should also be built to meet the demand when solar and wind energy are either absent or insufficient.

6. CONCLUSIONS

(1) Weather at SPM between October 2004 and July 2008 was characterized by very dry conditions between April and June (90% of the time the humidity was under 50%), wind speeds that tended to decrease between March and November, picking up in the winter months, and temperatures variations close to 2, 6 and 16°C during the night, for an entire day and for a whole year respectively. Wind speed was larger during the night and decreased steadily between sunrise and sunset, when the relative humidity was somewhat larger. Wind flowing from the south and south-southeast tended to be associated to warmer and more humid weather, higher pressure and lower solar irradiation than wind coming from the west and west-southwest.

(2) We obtained the parameters describing the behavior of wind speed as a function of height above ground level at a site that is relatively close to OAN telescopes. This information is useful for structural design and wind farm planning at SPM.

(3) The carbon footprint of the observatory under normal circumstances was close to 750 tons of

CO_2^{eq} a year, three times more than a typical mid-size industry in Ensenada, the district where OAN is located. The typical carbon footprint of a transport unit in the observatory was 17 kg(CO_2^{eq})/day, roughly 10% more than an average vehicle in Ensenada, a difference that can well be due to measurement errors. The production of 1 kWh for electricity at OAN emitted 1.2 kg(CO_2^{eq}), substantially more than in Ensenada, Baja California and Mexico (0.85, 0.57 and 0.78 kg(CO_2^{eq}) per kWh respectively). This is expected since conventional and inefficient diesel power plants produce electricity at SPM.

(4) Wind energy could have been harvested at SPM $\sim$ 60% of the time. Conditions were very good in February and less propitious in October, when wind could have been used during less than half of the time and was roughly ten times less powerful than in February. Conditions to extract wind energy were better at night. The amount of time that wind could have been harvested decreased during the day, with a minimum of $\sim$ 50% after sunset, when the wind power density was 4 times less than at dawn. More than half of the useful wind power flowed from the south and south-southwest, and nearly a fourth came from the north and north-northeast. This implies that wind turbines, if they are ever used in SPM, should probably be aligned in a NW-SE axis.

(5) It is likely that the energy requirements of OAN, roughly 110 kWh at peak demand, can be easily fulfilled using wind and solar energy. The daily and seasonal power consumption at the observatory should be analyzed in order to determine the best way to combine these two power sources.

(6) If the observatory is to remain isolated from the electric power grid, chemical or thermal units storing excess energy produced by wind and solar power are required in order to guarantee energy supply 100% of the time. An alternative possibility is a hybrid wind/solar/diesel system (an example of such a system can be seen at `www.danvest.com/winddieselsystems/`). If the observatory is connected to the grid, electric energy can be sold to the power company when supply exceeds demand, and bought when the opposite is true.

(7) The observatory spends close to 150,000 US$ a year for energy use (fuel, parts, service, etc.). This does not include the damage that is being caused to the environment, an externality that has to be accounted for in monetary terms. Two wind turbines, each capable of providing for the present annual energy needs of the observatory at peak consumption, cost close to 2 million US$. The price of a single solar energy plant, thermal or photovoltaic, is not higher than this. Thus, notwithstanding energy backup facilities, the initial investment for a solar plus wind energy system would be recovered in 25 years or so, assuming that fuel prices are stable during this period.

(8) Any decision regarding the power sources that best suit energy requirements at OAN should be preceded by decade-long development scenarios and policies for the observatory, since the amortization of energy investments takes a long time, as well as operational and technical policies to increase energy efficiency, since most of the energy spent at OAN is not for telescopes.

This paper would have been impossible without the dedication, professionalism and generosity of the TMT and LSST site testing teams. We appreciate the cooperation of the technical and administrative staff of OAN, and in particular the labor of Tomás Calvario, Osiris Escoboza, Francisco Guillén and Francisco Lazo. José Carlos Avelar, Desiderio Carrasco and Marco Mostalac assisted us with valuable information regarding energy use at OAN. We also thank Dr. Thomas Schlatter for his guidance regarding water vapor saturation pressure algorithms. The paper was benefited by comments and suggestions made by an anonymous referee. Support from DGAPA-Universidad Nacional Autónoma de México project IN102607-3 is gratefully acknowledged.

REFERENCES

Álvarez, M., Michel, R., Reyes-Coca, S., & Troncoso-Gaytán, R. 2007, RevMexAA (SC), 31, 111

Bohigas, J., et al. 2008, RevMexAA, 44, 231

Bolton, D. 1980, Monthly Weather Review 108, 1046

Erasmus, D. A., & van Staden, C. A. 2002, A Satellite Survey of Cloud Cover and Water Vapor in the Southwestern USA and Northern Mexico. A Study Conducted by CELT Project (Pasadena: Caltech)

Schöck, M., et al. 2009, PASP, 121, 384

Tapia, M., Hiriart, D., Richer, M., & Cruz-González, I. 2007, RevMexAA (SC), 31, 47

Wallace, J. M., & Hobbs, P. V. 2006, Atmospheric Science: An Introductory Survey (2nd ed.; San Diego, CA: Academic Press)

J. Bohigas and J. M. Núñez: Instituto de Astronomía, Universidad Nacional Autónoma de México, Apdo. Postal 877, 22800 Ensenada, B. C., México (jbb, jnunez@astrosen.unam.mx).